Numerical analysis on the traveling pulse in a kinetic chemotaxis model

Shugo YASUDA *

Graduate school of simulation studies,

University of Hyogo, Kobe 650-0047, Japan.

Abstract

A kinetic transport equation for chemotactic bacteria, i.e., a kinetic chemotaxis equation, coupled with reaction-diffusion equations for chemoattractants is considered. The Keller-Segel type equation for the population density of bacteria is derived by the asymptotic analysis of the kinetic chemotaxis equation in the continuum limit, where the ratio of the mean run length of bacteria to the characteristic length of the system, i.e., the Knudsen number, vanishes. Monte Carlo (MC) simulations of the kinetic chemotaxis model are performed for the traveling pulse problem with variation in the Knudsen number. The results of MC simulations are numerically compared with the Keller-Segel type equation. It is found that the results of MC simulations approach to that of the Keller-Segel type equation as decreasing the Knudsen number. However, a significant difference still remains for moderately small Knudsen numbers which correspond to the micro scale systems. This result demonstrates an importance of the kinetic chemotaxis model in the micro scale systems.

Keywords: Kinetic transport equation, chemotaxis, run-and-tumble, traveling pulse, Monte Carlo simulation

* Electronic mail: yasuda@sim.u-hyogo.ac.jp

I. INTRODUCTION AND BASIC EQUATION

We consider the chemotactic bacteria who create the run-and-tumble motions, e.g., *E. Coli*[1–4], where the bacteria run linearly with a constant speed when rotating their flagella in counter-clockwise direction, but occasionally change the running direction (tumble) when rotating their flagella in clockwise direction. The bacteria also change their tumbling frequencies according to the variations of chemical attractants along their pathways; they increase the tumbling frequency when moving toward a lower-concentration region of chemoattractants while decrease the tumbling frequency when moving toward a higher-concentration region of chemoattractants. This chemotactic behaviors (or chemotaxis) create the biased random motions searching for the higher concentrations of chemoattractants. The density of the chemotactic bacteria with a velocity v at a position x and a time t, $f(t, x, v)$, is described by the kinetic transport equation incorporating the chemotactic response function of the bacteria, say the kinetic chemotaxis model. The kinetic transport equation is also coupled with the reaction-diffusion equations for chemoattractants. The kinetic chemotaxis model was first proposed in [5] and has been further developed toward involving the detailed microscopic mechanism in the chemotaxis [6–9].

In this paper, we consider the kinetic chemotaxis equation incorporating the chemotactic response function which depends on the temporal variations of chemoattractants along the pathway of each bacterium. The kinetic chemotaxis equation is coupled with the reaction-diffusion equations for two chemoattractants; one is a nutrient consumed by the bacteria, whose concentration at a position x and a time t is written as $N(t, x)$, and the other is a secretion produced by the bacteria, whose concentration is written as $S(t, x)$. Then, the kinetic chemotaxis equation is written as

$$\partial_t f(t, x, v) + v \cdot \nabla_x f(t, x, v) = \psi_0 \left\{ \int_{|v'|=V_0} \Psi(v') K(v, v') f(v') dv' - \Psi(v) f(v) \right\} + P[\rho] f(v), \tag{1}$$

where ψ_0 is the mean tumbling frequency, $P[\rho]$ is the proliferation rate (which may depend on the local population density of bacteria ρ), $\Psi(v)$ is the chemotactic response function (defined in Eq. (3)), and $K(v, v')$ is the probability density of the reorientation angle that

the bacteria with velocity $\boldsymbol{v}'$ get a new velocity $\boldsymbol{v}$ in the tumbling and satisfies

$$\int_{|v|=V_0} K(\boldsymbol{v},\boldsymbol{v}')d\boldsymbol{v}' = 1. \tag{2}$$

Note that, in Eqs. (1) and (2), we consider that the bacteria has a constant speed V_0, so that the integration as to velocity $\boldsymbol{v}$ is performed over the surface of the sphere with radius V_0. The response function $\Psi(\boldsymbol{v})$ describes the bias of tumbling frequency of the bacteria with a velocity $\boldsymbol{v}$ and defined as

$$\Psi(\boldsymbol{v}) = 1 - \frac{\chi_S}{2}\tanh\left(\frac{1}{\delta}\frac{D\log S}{Dt}\bigg|_v\right) - \frac{\chi_N}{2}\tanh\left(\frac{1}{\delta}\frac{D\log N}{Dt}\bigg|_v\right), \tag{3}$$

where δ^{-1} is the stiffness parameter in the response, χ_S and χ_N are the modulations in the responses to S and N, respectively, and $\frac{D}{Dt}|_v$ is the material derivative with velocity $\boldsymbol{v}$, i.e., $\frac{D}{Dt}|_v = \partial_t + \boldsymbol{v}\cdot\nabla_x$.

The concentrations of chemoattractants S (which is produced by the bacteria) and N (which is consumed by the bacteria) are described by the following reaction-diffusion equations:

$$\partial_t S(t,\boldsymbol{x}) = D_S\Delta S - aS + b\rho, \tag{4}$$

$$\partial_t N(t,\boldsymbol{x}) = D_N\Delta N - cN\rho, \tag{5}$$

where D_S and D_N are the diffusion constants, a is the degradation rate of S, b and c are the production rate of S and consumption rate of N by the bacteria, respectively, and ρ is the population density of bacteria, which is calculated as

$$\rho(t,\boldsymbol{x}) = \frac{1}{4\pi V_0^2}\int_{|v|=V_0} f(t,\boldsymbol{x},\boldsymbol{v})d\boldsymbol{v}. \tag{6}$$

In non-dimensional form, we scale the microscopic velocity $\boldsymbol{v}$ by the constant speed of bacteria V_0, the space $\boldsymbol{x}$ by an arbitrary characteristic length L_0, the time t by a characteristic time t_0 (which is given in Eq. (8), and the proliferation rate P by t_0^{-1}. We also introduce a non-dimensional parameter k which is defined by the ratio of the mean run length of bacteria, $V_0\psi_0^{-1}$, to the characteristic length, i.e.,

$$k = \frac{V_0\psi_0^{-1}}{L_0}. \tag{7}$$

The non-dimensional parameter k corresponds to the Knudsen number in the rarefied gas dynamics. The macroscopic equations can be derived from the kinetic equation by the asymptotic analysis when k is small.

When we take the characteristic time t_0 as

$$t_0 = L_0/(kV_0), \tag{8}$$

the non-dimensional form of the kinetic chemotaxis equation is written as

$$k^2\frac{\partial \hat{f}}{\partial \hat{t}} + k\hat{\boldsymbol{v}} \cdot \nabla_{\hat{\boldsymbol{x}}}\hat{f} = \int_{|\hat{\boldsymbol{v}}|=1} \Psi(\hat{\boldsymbol{v}}')\hat{K}(\hat{\boldsymbol{v}}, \hat{\boldsymbol{v}}')\hat{f}(\boldsymbol{v}')d\Omega(\hat{\boldsymbol{v}}) - \Psi(\hat{\boldsymbol{v}})\hat{f}(\hat{\boldsymbol{v}}) + k^2\hat{P}[\hat{\rho}]\hat{f}(\hat{\boldsymbol{v}}). \tag{9}$$

Hereafter " ^ " indicates the non-dimensionalized quantities. The density f and population density ρ are both scaled by a reference population density ρ_0 and where $\hat{\rho}$ is given by the integration of $\hat{f}$ as

$$\hat{\rho}(\hat{t}, \hat{\boldsymbol{x}}) = \frac{1}{4\pi}\int_{|\hat{\boldsymbol{v}}|=1} \hat{f}(\hat{t}, \hat{\boldsymbol{x}}, \hat{\boldsymbol{v}})d\Omega(\hat{\boldsymbol{v}}). \tag{10}$$

The non-dimensional equations for S and N are written as

$$\frac{\partial \hat{S}}{\partial \hat{t}} = \hat{D}_S\hat{\Delta}\hat{S} - \hat{a}\hat{S} + \hat{\rho}, \tag{11}$$

$$\frac{\partial \hat{N}}{\partial \hat{t}} = \hat{D}_N\hat{\Delta}\hat{N} - \hat{c}\hat{N}\hat{\rho}, \tag{12}$$

where S is scaled by $t_0\rho_0 b$, N by an arbitrary reference quantity N_0, D_S and D_N by L_0^2/t_0, a by t_0^{-1}, and c by $(\rho_0 t_0)^{-1}$.

The stiffness in the response function δ^{-1} is scaled as

$$\hat{\delta} = \frac{\delta}{V_0/L_0}. \tag{13}$$

Equation (13) also prescribes the characteristic length L_0 as $L_0 \sim \mathcal{O}(V_0\delta^{-1})$. This indicates that the characteristic length L_0 considered in this paper corresponds to the length scale which is generated by the chemotactic response of the bacteria moving with a constant speed V_0.

In the following text, we solely use the non-dimensional quantities defined in this section and omit " ^ " in the notations of non-dimensional quantities.

II. ASYMPTOTIC ANALYSIS

The continuum equations to describe the population density of chemotactic bacteria, e.g., the Keller-Segel equation [10, 11], are derived by the asymptotic analysis of the kinetic chemotaxis equation.[12–14] In this section we derive the Keller-Segel type equation for the

population density of bacteria by the asymptotic analysis of the kinetic chemotaxis model Eq. (9) in the continuum limit $k \to 0$. In the following text, we solely consider the uniform scattering, i.e., $K = 1/4\pi$, and small modulation parameters in the response function as

$$\chi_S = k\phi_S, \quad \chi_N = k\phi_N. \tag{14}$$

Thus, the kinetic chemotaxis equation is written as

$$k^2 \partial_t f + k\boldsymbol{v} \cdot \nabla f = \frac{1}{4\pi} \int_{|v|=1} \Psi(\boldsymbol{v}')f(\boldsymbol{v}')d\Omega(\boldsymbol{v}') - \Psi(\boldsymbol{v})f(\boldsymbol{v}) + k^2 P[\rho]f(\boldsymbol{v}), \tag{15}$$

with

$$\Psi(\boldsymbol{v}) = 1 - k\left\{ \frac{\phi_S}{2} \tanh\left(\frac{k\partial_t \log S + \boldsymbol{v} \cdot \nabla \log S}{\delta} \right) + \frac{\phi_N}{2} \tanh\left(\frac{k\partial_t \log N + \boldsymbol{v} \cdot \nabla \log N}{\delta} \right) \right\}. \tag{16}$$

By substituting the expansions $f = f_0 + kf_1 + k^2 f_2 + \cdots$ and $\Psi = 1 - k\Psi_1 - k^2\Psi_2 + \cdots$, we obtain the following equation,

$$\begin{aligned}
k\boldsymbol{v} \cdot \nabla f_0 &+ k^2 \left(\partial_t f_0 + \boldsymbol{v} \cdot \nabla f_1 \right) \\
&= \frac{1}{4\pi} \int f_0(\boldsymbol{v}')d\Omega(\boldsymbol{v}') - f_0(\boldsymbol{v}) \\
&+ k\left\{ \frac{1}{4\pi} \int [f_1(\boldsymbol{v}') - \Psi_1(\boldsymbol{v}')f_0(\boldsymbol{v}')] \, d\Omega(\boldsymbol{v}') - [f_1(\boldsymbol{v}) - \Psi_1(\boldsymbol{v})f_0(\boldsymbol{v})] \right\} \\
&+ k^2 \left\{ \frac{1}{4\pi} \int [f_2(\boldsymbol{v}') - \Psi_1(\boldsymbol{v}')f_1(\boldsymbol{v}') - \Psi_2(\boldsymbol{v}')f_0(\boldsymbol{v}')] \, d\Omega(\boldsymbol{v}') \right. \\
&\left. - [f_2(\boldsymbol{v}) - \Psi_1(\boldsymbol{v})f_1(\boldsymbol{v}) - \Psi_2(\boldsymbol{v})f_0(\boldsymbol{v})] + P[\rho_0]f_0(\boldsymbol{v}) \right\} + \mathcal{O}(k^3). \tag{17}
\end{aligned}$$

For the k^0 terms in Eq. (17), we find that $f(\boldsymbol{v})$ is constant as to $\boldsymbol{v}$, so that, from Eq. (10), we obtain

$$f_0(t, \boldsymbol{x}, \boldsymbol{v}) = \rho_0(t, \boldsymbol{x}). \tag{18}$$

The equation for $\rho_0(t, \boldsymbol{x})$ is obtained by integrating Eq. (15) as to $\boldsymbol{v}$, i.e.,

$$\partial_t \rho_0 + \nabla \cdot \boldsymbol{J_1} = P[\rho_0]\rho_0, \tag{19}$$

where

$$\boldsymbol{J_1} = \frac{1}{4\pi} \int_{|v|=1} \boldsymbol{v} f_1(\boldsymbol{v})d\Omega(\boldsymbol{v}). \tag{20}$$

For k^1 terms in Eq. (17), we have

$$\boldsymbol{v} \cdot \nabla \rho_0 = \frac{1}{4\pi} \int_{|v|=1} [f_1(\boldsymbol{v}') - \Psi_1(\boldsymbol{v}')\rho_0]d\Omega(\boldsymbol{v}') - [f_1(\boldsymbol{v}) - \Psi_1(\boldsymbol{v})\rho_0]. \tag{21}$$

By integrating the above equation multiplied by $\boldsymbol{v}$, we obtain

$$\boldsymbol{J}_1 = -\frac{1}{3}\nabla\rho_0 + \boldsymbol{U}[\nabla S, \nabla N]\rho_0, \tag{22}$$

where

$$\boldsymbol{U}[\nabla S, \nabla N] = \frac{1}{4\pi}\int_{|\boldsymbol{v}|=1}\boldsymbol{v}\Psi_1(\boldsymbol{v})d\Omega(\boldsymbol{v}). \tag{23}$$

Here we use $\int_{|\boldsymbol{v}|=1}v_\alpha v_\beta d\Omega(\boldsymbol{v}) = \frac{4\pi}{3}\delta_{\alpha\beta}$, where $\delta_{\alpha\beta}$ is the Kronecker delta.

From Eq. (16), Ψ_1 is written as

$$\Psi_1(\boldsymbol{v}) = \sum_{F=S,N}\frac{\phi_F}{2}\tanh\left(\frac{\boldsymbol{v}\cdot\nabla\log F}{\delta}\right). \tag{24}$$

Thus, $\boldsymbol{U}[\nabla S, \nabla N]$ is calculated as

$$\boldsymbol{U}[\nabla S, \nabla N] = \sum_{F=S,N}\frac{\phi_F}{8\pi}\int_{|\boldsymbol{v}|=1}\boldsymbol{v}\tanh\left(\frac{\boldsymbol{v}\cdot\nabla\log F}{\delta}\right)d\Omega(\boldsymbol{v}), \tag{25a}$$

$$= \sum_{F=S,N}\frac{\phi_F}{4}\frac{\nabla\log F}{|\nabla\log F|}\int_{-1}^{1}w\tanh\left(\frac{w|\nabla\log F|}{\delta}\right)dw. \tag{25b}$$

Finally, we obtain the reaction-diffusion-drift equation for the population density ρ_0, i.e.,

$$\partial_t\rho_0 + \nabla(U[\nabla S, \nabla N]\rho_0) = \frac{1}{3}\Delta\rho_0 + P[\rho_0]\rho_0, \tag{26}$$

where $U[\nabla S, \nabla N]$, which is written in Eq. (25), represents the drift generated by the chemotactic responses of bacteria.

III. NUMERICAL RESULTS

In this section, presented are the numerical results obtained in [15], where the traveling pulse of the population density of bacteria in a micro channel is investigated by Monte Carlo (MC) simulations for the kinetic chemotaxis model. The MC results are also numerically compared with the Keller-Segel type equation obtained by the asymptotic analysis of the kinetic chemotaxis model. The geometry of MC simulation is shown in Fig. 1, where the uniform lattice-mesh system is used to calculated the chemoattractants S and N, i.e., Eqs. (11) and (12), by a finite volume scheme and MC particles (which represent each bacterium) are distributed in each lattice site. The MC particles are initially accumulated in the vicinity of $x = 0$ while the concentration of nutrient N is uniformly distributed as $N = 1$ and that
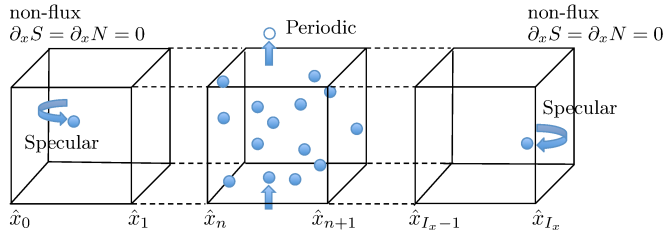
FIG. 1: The geometry of Monte Carlo simulation. The motions of bacteria are calculated by the MC particles while the concentrations of chemoattractants are calculated by the finite volume scheme on the uniform lattice-mesh system. The specular reflection condition for the MC particles and the non-flux condition for chemoattractants are considered at left- and right-side walls in the channel while the periodic conditions are considered for both MC particles and chemical cues in y and z directions. [Figure 1 in [15] is reused.]

TABLE I: The values of parameters.

Degradation rate a	24.0
Consumption rate c	120.0
Diffusion coefficient D_S	3.84
Diffusion coefficient D_N	3.84
Modulation parameter ϕ_S	24.0
Modulation parameter ϕ_N	72.0
Stiffness parameter δ^{-1}	0.2

of secretion S is uniformly zero initially. For more details in the MC method, one can refer [15]. In the following of text, we only consider the non-proliferation case, $P[\rho_0] = 0$.

The Monte Carlo simulations are carried out with variations in k, i.e., k=0.02, 0.01, 0.005, 0.002, and 0.001, whereas the values of other parameters are fixed as shown in Table I, where the parameters' values are chosen so as to correspond to the experimental measurements in [?]. The drift-diffusion equation for the population density of bacteria, i.e., Eq. (26) with $P = 0$, is numerically calculated with the finite volume method in the one-dimensional extent, where flux U, Eq. (25) (x component), is also calculated at each time step by using the Simpson's integral method according to the gradients of chemoattractants obtained at the previous time step. To obtain the accurate results for small values of k (or large tumbling
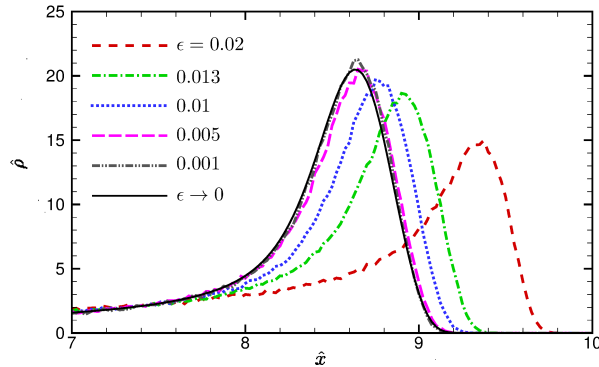
FIG. 2: Comparison of the population densities of bacteria for different values of k and for the asymptotic limit at time $t = 0.5$. ϵ in the figure corresponds to k in the text. [Figure 12 in [15] is reused.]

frequencies ψ_0) in Monte Carlo simulations, the time-step size Δt and particle number M are set sufficiently small and sufficiently large, respectively, as $\Delta \hat{t} = 1 \times 10^{-4}$ and $M = 226560$. For the numerical accuracy tests, please refer [15].

Figure 2 shows the snapshots of the population density of bacterial obtained by the MC simulations with variation in k and that obtained by the finite volume calculation of Eq. (26) and (25). It is seen that the results of MC simulations are asymptotically close to the asymptotic solution in the continuum limit as k decreases; the snapshot of the population density for $k = 0.001$ obtained by the Monte Carlo simulation almost coincides with the asymptotic solution in the continuum limit. However, significant deviations from the asymptotic solution are still observed for moderately small values of k, i.e., $\epsilon \gtrsim 0.01$.

Figure 3 shows the convergence of the traveling speed $\hat{V}_{\text{wave}}$ scaled by k in the continuum limit $\epsilon \to 0$. It is seen that as increasing the stiffness parameter δ^{-1}, the results obtained with Eq. (3) converges to those obtained with the sign response function and the result of the sign response function converges to that obtained by the analytical formula in Ref. [17] in the continuum limit $k \to 0$. This also demonstrates that the MC method can accurately reproduce the analytical result of the traveling speed obtained in Ref. [17].

It should be noted that the parameter k depends not only on the biological properties of bacteria but also on the characteristic length L_0 of the system. Thus, the parameter k becomes significant when we consider, for example, the cluster formation of bacteria in
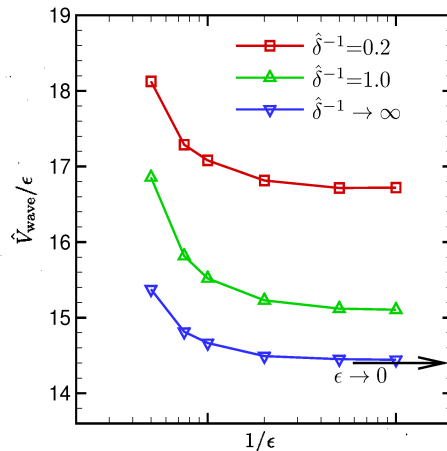
FIG. 3: The traveling speed of the population pulse vs. the inverse of k for different stiffness parameters. For $\delta^{-1} \to \infty$, the hyperbolic tangent in Eq. (3) is replaced with the sign function $\hat{X}/|\hat{X}|$. The left arrow shows the traveling speed for $\delta^{-1} \to \infty$ in the continuum limit obtained by the analytical formula in [17]. ϵ in the figure corresponds to k in the text. [Figure 13 in [15] is reused.]

the micro devices, in which the characteristic length L_0 should be small. In fact, the mean tumbling frequency ψ_0 and constant speed V_0 of bacteria are measured as $\psi_0 = 3.0$ [1/s] and $V_0 = 25$ [μm/s] in [16]. Thus, when we consider a micro system with characteristic length $L_0 = 500$ [μm], the non-dimensional parameter k is calculated as k=0.017. We remark that the deviation between the kinetic and Keller-Segel equations is obviously observed in both population density profile and traveling speed for the above value of k. The deviations observed for moderately-small values of k indicate that the kinetic chemotaxis model can take on a significance in the investigation on the micro scale systems. This result also demonstrates the restriction of the continuum model (e.g., Keller-Segel type equation) and the importance of the kinetic chemotaxis model in the investigation on the micro-scale systems with moderately-small values of k.

[1] J. Adler, "Chemotaxis in bacteria", Annu. Rev. Biochem. **44**, 341 (1975).

[2] E. O. Budrene and H. C. Berg, "Complex patterns formed by motile cells of Escherichia coli",

Nature **349**, 630 (1991).

[3] E. O. Budrene and H. C. Berg, "Dynamics of formation of symmetrical patterns by chemotactic bacteria", Nature **376**, 49 (1995).

[4] H. C. Berg, *E. Coli in Motion* (Springer, Berlin, 2003).

[5] H. G. Othmer, S. R. Dunbar, and W. Alt, "Models of dispersal in biological systems", J. Math. Biol. **26**, 263 (1988).

[6] R. Erban and H. G. Othmer, "From individual to collective behavior in bacterial chemotaxis", SIAM J. Appl. Math. **65**, 361 (2004).

[7] Y. Dolak and C. Schmeiser, "Kinetic models for chemotaxis: Hydrodynamic limits and spatio-temporal mechanisms", J. Math. Biol. **51**, 595 (2005).

[8] N. Bellomo, A. Bellouquid, J. Nieto, and J. Soler, "Multicellular biological growing systems: Hyperbolic limits towards macroscopic description", Math. Model Methods Appl. Sci. **17**, 1675–1693 (2007).

[9] B. Perthame, *Transport Equations in Biology* (Birkhäuser Verlag, Basel, 2007).

[10] E. F. Keller and L. A. Segel, "Model for Chemotaxis", J. Theor. Biol. **30**, 225 (1971).

[11] E. F. Keller and L. A. Segel, "Traveling bands of chemotactic bacteria: a theoretical analysis", J. Theor. Biol. **30**, 235 (1971).

[12] T. Hillen and H. G. Othmer, "The diffusion limit of transport equations derived from velocity-jump processes", SIAM J. Appl. Math. **61**, 751 (2000).

[13] H. Othmer and T. Hillen, "The diffusion limit of transport equations. II. Chemotaxis equations", SIAM J. Appl. Math. **62**, 1222 (2002).

[14] F. A. C. C. Chalub, P. Markowich, B. Perthame, and C. Schmeiser, "Kinetic models for chemotaxis and their drift-diffusion limits", Monatsh. Math. **142**, 123 (2004).

[15] S. Yasuda, "Monte Carlo simulation for kinetic chemotaxis model: An application to the traveling population wave", J. Comput. Phys. **330**, 1022–1042 (2017).

[16] J. Saragosti, V. Calvez, N. Bournaveas, B. Perthame, A. Buguin, and P. Silberzan, "Directional persistence of chemotactic bacteria in a traveling concentration wave", PNAS **108**, 16235 (2011).

[17] J. Saragosti, V. Calvez, N. Bournaveas, A. Buguin, P. Silberzan, and B. Perthame, "Mathematical Description of Bacterial Traveling Pulses", PLoS Comput. Biol. **6**, e1000890 (2010).